THE JOURNAL OF PHYSICAL CHEMISTRY LETTERS
A JOURNAL OF THE AMERICAN CHEMICAL SOCIETY

pubs.acs.org/JPCL Letter

Over 20% Carbon-13 Polarization of Perdeuterated Pyruvate Using Reversible Exchange with Parahydrogen and Spin-Lock Induced Crossing at 50 μT

Andreas B. Schmidt,* James Eills, Laurynas Dagys, Martin Gierse, Michael Keim, Sebastian Lucas, Michael Bock, Ilai Schwartz, Maxim Zaitsev, Eduard Y. Chekmenev, and Stephan Knecht*

Cite This: *J. Phys. Chem. Lett.* 2023, 14, 5305−5309 Read Online

ACCESS | Metrics & More | Article Recommendations | Supporting Information

ABSTRACT: Carbon-13 hyperpolarized pyruvate is about to become the next-generation contrast agent for molecular magnetic resonance imaging of cancer and other diseases. Here, efficient and rapid pyruvate hyperpolarization is achieved via signal amplification by reversible exchange (SABRE) with parahydrogen through synergistic use of substrate deuteration, alternating, and static microtesla magnetic fields. Up to 22 and 6% long-lasting ^{13}C polarization (T_1 = 3.7 ± 0.25 and 1.7 ± 0.1 min) is demonstrated for the C1 and C2 nuclear sites, respectively. The remarkable polarization levels become possible as a result of favorable relaxation dynamics at the microtesla fields. The ultralong polarization lifetimes will be conducive to yielding high polarization after purification, quality assurance, and injection of the hyperpolarized molecular imaging probes. These results pave the way to future *in vivo* translation of carbon-13 hyperpolarized molecular imaging probes prepared by this approach.

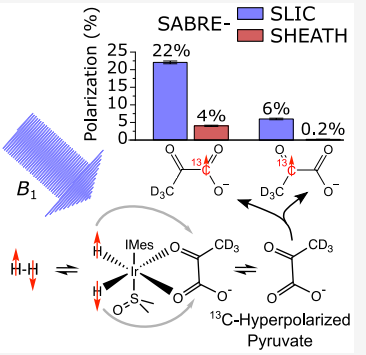

Hyperpolarized (HP) ^{13}C-pyruvate is being used as a contrast agent in clinical trials, because its metabolic flux can be tracked non-invasively and temporally resolved using magnetic resonance imaging (MRI).[1] This carries valuable diagnostic information, because abnormal pyruvate metabolism is associated with various pathologies (e.g., tumor cells exhibit accelerated pyruvate-to-lactate conversion,"Warburg effect").[2] Pyruvate has emerged as the leading HP MRI agent because of fast cellular uptake and its central position in cellular metabolism at the cross-section of glycolysis, the citric acid cycle, alanine transamination, and lactate fermentation.[3] HP pyruvate is under evaluation in over 30 clinical trials as of 2022. In almost all cases [1-^{13}C]pyruvate is used, but [2-^{13}C]-pyruvate has recently been demonstrated in humans with the advantage that the C2 atom enters the citric acid cycle.[4] The leading technology for HP pyruvate is dissolution dynamic nuclear polarization (dDNP).[5] However, it is expensive (~2M €) and low-throughput (~1 h per sample). More cost-effective and faster technologies are needed for future widespread clinical utilization.

Duckett and co-workers have pioneered a "non-hydrogenative" parahydrogen (pH_2)-based hyperpolarization approach referred to as signal amplification by reversible exchange (SABRE).[6−8] It relies on reversible, simultaneous binding of pH_2, which is the nuclear spin-singlet isomer of molecular hydrogen, and the target molecule to an iridium-based exchange complex.[9] Recently, SABRE was used to produce HP pyruvate,[10] with $P_{^{13}C} \approx 10\%$ for [1-^{13}C]pyruvate and $P_{^{13}C} \approx 1\%$ for [2-^{13}C]pyruvate.[11,12] In another important step, the extraction of highly polarized ($P_{^{13}C} \approx 9\%$) [1-^{13}C]pyruvate into aqueous solution after precipitation from methanol was shown, paving the way to future biomedical MRI studies with SABRE-polarized pyruvate.[13]

In SABRE, polarization transfer from pH_2 to ^{13}C is mediated by the indirect dipolar couplings (J couplings) between nuclei in the transient complexes 2 and 2′ shown in Figure 1b. For SABRE, the ultralow magnetic field regime (hundreds of nanoteslas) plays an important role. At these fields, nuclear spin energy states of the molecules are matching and the J-coupling interaction effectively perturbs the eigenstates, such that energy level crossing is avoided [level anticrossing (LAC)].[14] When a SABRE reaction is carried out at the LAC, the target ^{13}C spin is spontaneously hyperpolarized.[15−17] This method is called SABRE-SHEATH (SABRE in shield enables alignment transfer to heteronuclei) and has been demonstrated for [1-^{13}C]pyruvate. More recently, pulsed static fields have been used to induce this effect, delivering similar ^{13}C polarization ($P_{^{13}C}$) of HP [1-^{13}C]pyruvate as SABRE-SHEATH.[18−21] Pulsed radio frequency (rf) fields can be employed for polarization transfer.[22,23] Spin-lock induced

Received: March 16, 2023
Accepted: May 22, 2023

https://doi.org/10.1021/acs.jpclett.3c00707
J. Phys. Chem. Lett. 2023, 14, 5305−5309

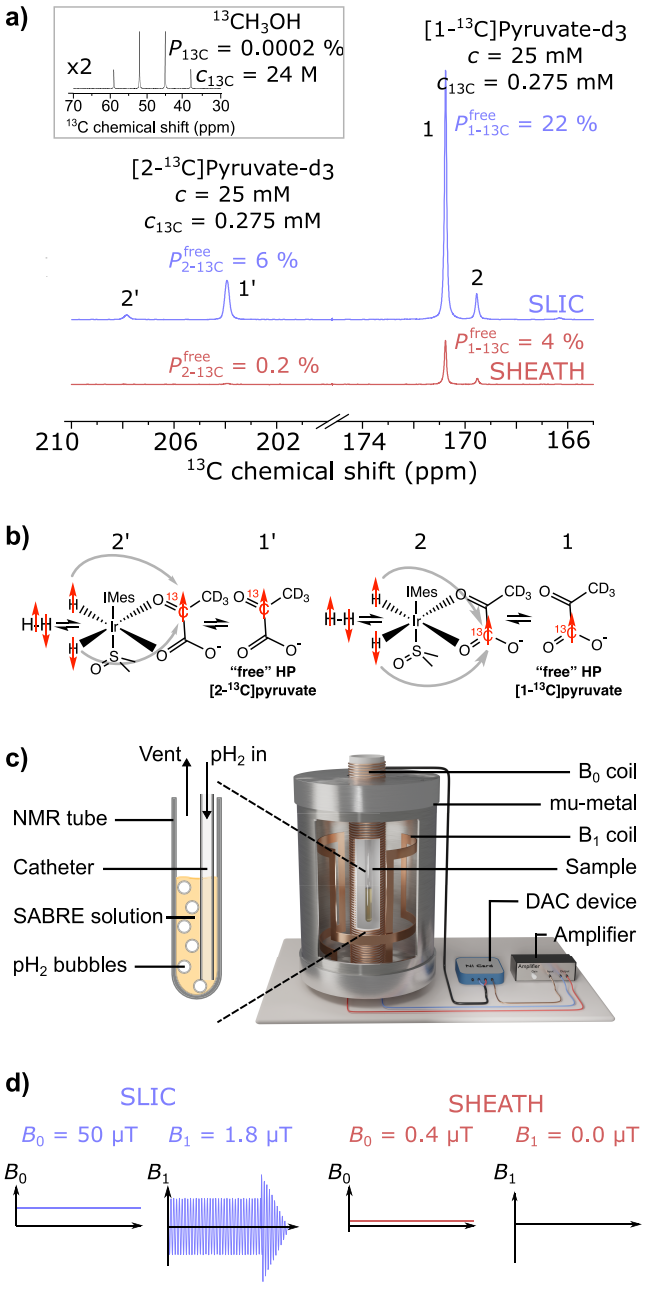

Figure 1. (a) ^{13}C NMR spectra of SLIC-SABRE and SABRE-SHEATH hyperpolarization of [1-^{13}C]- and [2-^{13}C]pyruvate-d_3. The inset displays the ^{13}C NMR reference spectrum of a ^{13}C-enriched sample of non-hyperpolarized neat methanol. (b) Exchange reaction occurring between the Ir-based organometallic complex, free parahydrogen, and free pyruvate in solution. (c) Experimental setup used for hyperpolarization experiments keeping the SABRE sample at ∼3−7 °C, constant magnetic field (B_0), and SLIC rf field (B_1). A schematic magnification of the NMR tube during pH_2 bubbling is shown on the left, and a rendering of the complete setup is displayed on the right. Panel c was adapted with permission from ref 31. Copyright 2023 American Chemical Society. (d) SLIC-SABRE and SABRE-SHEATH protocols used in this work.

crossing (SLIC) by continuous rf irradiation at tesla fields has also been applied along with SABRE and was termed low-irradiation generation of high tesla- (LIGHT-) or SLIC-SABRE.[24−29] However, P^{13}_C values achieved by high-field SLIC-SABRE were found to be lower than those obtained via SABRE-SHEATH. The reason for these low P^{13}_C is that SLIC at tesla fields faces significant challenges: often unfavorable relaxation dynamics because of chemical shift anisotropy (CSA), singlet-to-triplet mixing of parahydrogen,[30] and a need for selective excitation of the bound and free SABRE species as a result of larger chemical shift dispersion. In sharp contrast, at microtesla fields, ^{13}C chemical shift differences are negligible and relaxation times become favorable.

Here, we show that SLIC-SABRE can be carried out at microtesla fields to quickly hyperpolarize [1-^{13}C]- and [2-^{13}C]pyruvate-d_3, producing high ^{13}C polarizations of P^{13}_C = 22 and 6%, respectively (Figure 1a). In comparison to the thermal equilibrium polarization of $P^{13}_C \approx 0.0002\%$ at the 1.9 T detection field, these P^{13}_C levels correspond to signal enhancements of 140 000- and 40 000-fold. To achieve these P^{13}_C levels, we performed the SABRE reaction (Figure 1b) by bubbling pH_2 through a solution of ∼30 mM pyruvate-d_3 in CD_3OD at 50 μT and ∼3−7 °C (Figure 1c) in the presence of a spin-lock induced crossing (SLIC) rf field (Figure 1d). Pyruvate-d_3 (and pyruvate-h_3 below) was used with natural ^{13}C abundance (1.1%) to minimize sample-to-sample variability; no difference in P^{13}_C values between ^{13}C-labeled and natural abundance samples was observed. After the SLIC process, an adiabatic 90° pulse was used to align the ^{13}C polarization longitudinally along the 50 μT field and the sample was moved from the SABRE setup to an 80 MHz benchtop nuclear magnetic resonance (NMR) system for HP ^{13}C signal acquisition. A detailed description of the setup and methods is reported in the Supporting Information.

These pyruvate polarization levels are 2−6 times higher than P^{13}_C values reported using SABRE before.[10−13,21] To better understand why SLIC-SABRE at microtesla fields shows such high efficacy, we carried out experiments using both protonated and deuterated pyruvate and using SLIC-SABRE and SABRE-SHEATH. The ^{13}C polarization levels are shown in Figure 2a. Protonated [1-^{13}C]- and [2-^{13}C]pyruvate show similar P^{13}_C values for both polarization protocols: 12 versus 9% for [1-^{13}C] and 2% in both cases for [2-^{13}C]pyruvate. However, we found that SLIC-SABRE performed much better for pyruvate-d_3: P^{13}_C using SABRE-SHEATH (at 0.4 μT) was 4 and 0.2% for [1-^{13}C]- and [2-^{13}C]pyruvate-d_3, respectively, but increased to 22 and 6% with SLIC-SABRE.

The rationale behind these observations is that the deuterium nuclei have two distinct effects on relaxation. First, at ultralow fields, the deuterons are strongly coupled to the ^{13}C spins and act as a quadrupolar relaxation sink.[17] This is the case during SABRE-SHEATH and is particularly detrimental for C2 carbon, which has stronger J couplings to the deuterons than C1. Their second effect is to reduce the rate of intramolecular dipole−dipole relaxation experienced by the ^{13}C spins because the magnetic moments of deuterons are smaller than those of protons. This effect manifests in the higher ^{13}C polarizations and more favorable polarization buildup kinetics, which are shown in Figure 2b. To support this hypothesis, we also present measured T_1 and $T_{1\rho}$ values and find that $T_{1\rho}$ at 50 μT is longer than T_1 at 0.4 μT for all investigated pyruvate isotopologues (Figure 2c), ultimately enabling effective polarization buildup. Thus, for the pyruvate-d_3 isotopologues for which T_1 under SABRE-SHEATH and $T_{1\rho}$ under SLIC-SABRE conditions differ the most, much higher polarizations are achieved with SLIC-SABRE. We envision that further analysis of the polarization transfer in the SABRE exchange complex during SLIC and experimental parameter optimization (mostly reaction temperature, static

https://doi.org/10.1021/acs.jpclett.3c00707
J. Phys. Chem. Lett. 2023, 14, 5305−5309

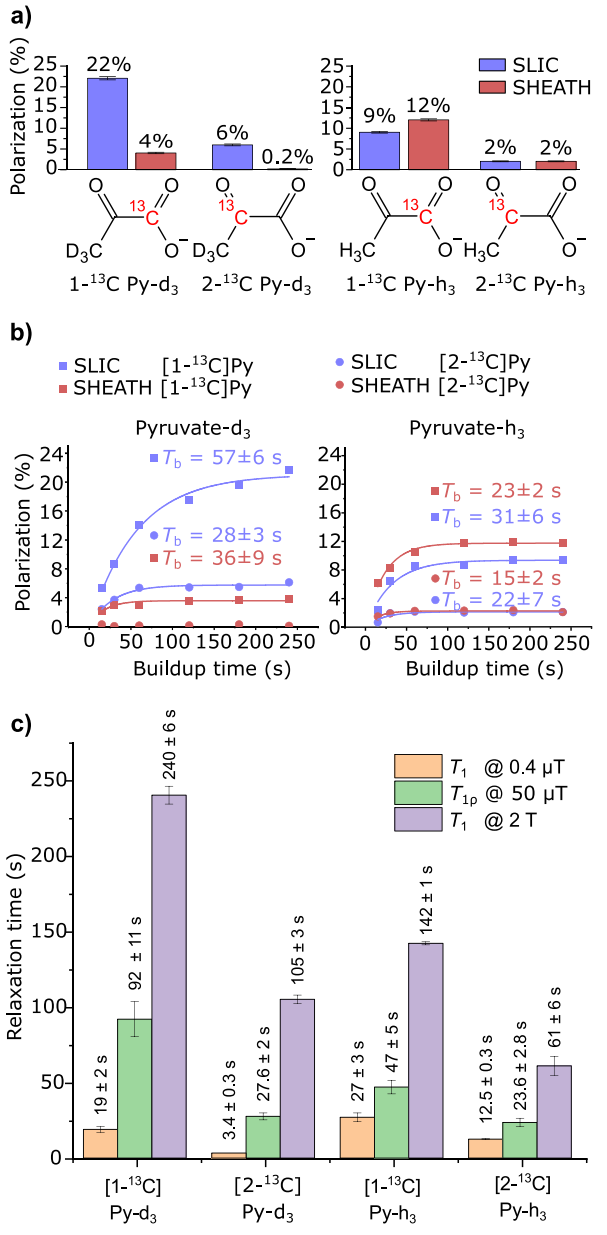

Figure 2. (a) SLIC-SABRE and SABRE-SHEATH hyperpolarization yields of [1-^{13}C]pyruvate-d_3 (Py-d_3), [2-^{13}C]Py-d_3, [1-^{13}C]pyruvate (Py-h_3), and [2-^{13}C]Py-h_3. (b) Polarization buildup dynamics of SLIC-SABRE and SABRE-SHEATH. (c) Relevant relaxation times of ^{13}C hyperpolarization under SABRE-SHEATH conditions at 0.4 μT (T_1), SLIC-SABRE conditions at 50 μT ($T_{1\rho}$), and T_1 at the NMR detection field of 1.9 T. Relaxation measurements were performed at room temperature. Detailed relaxation data are presented in Figures S6 and S7 of the Supporting Information. Error bars correspond to the standard deviation determined in N = 5 independent samples polarized under the same conditions (a; see the Supporting Information) or the fit error of the exponential curve fitting (b and c).

magnetic field, and SLIC rf field) will enable even greater signal enhancements.

Notably, deuterium isotope labeling can prolong T_1 relaxation also at clinical magnetic fields.[32] In Figure 2c, we show ^{13}C T_1 relaxation values for HP [1-^{13}C]- and [2-^{13}C]-pyruvate-d_3 measured in CD_3OD at 1.9 T and ambient temperature. We find C1 $T_1 \rightarrow$ 223 ± 16 s and C2 $T_1 \rightarrow$ 102 ± 4 s versus C1 → 137 ± 6 s and C2 → 56 ± 6 s for the deuterated and pronated forms, respectively. The longer polarization lifetime gained by deuteration is conducive to yielding high $P_{^{13}C}$ after purification, quality assurance, and injection of the HP contrast agent solution. Indeed, this important result has recently enabled us to perform the first *in vivo* metabolic imaging with purified aqueous SABRE-hyperpolarized [1-^{13}C]pyruvate-d_3 in mice in a follow-up study.[33]

While larger polarizations and lifetimes are advantageous, it is important to consider the applicability of hyperpolarized pyruvate-d_3 for monitoring biochemical reactions. In comparison to pyruvate-h_3, the deuteration leads to changes in the zero-point energy states of the molecule that can ultimately reflect in a kinetic isotope effect. Indeed, changes in the conversion rates have been reported for other hyperpolarized molecules, such as [2-^{2}H]alanine.[32] However, the effects are often small.[34,35] Particularly, for pyruvate, no significant deuterium isotope effect on metabolic conversion kinetics has been observed, meaning that, for metabolic HP MRI, pyruvate-d_3 can successfully be utilized instead of the non-deuterated variant.[36]

Notably, both isotope-enriched [1-^{13}C]- and [2-^{13}C]-pyruvate-d_3 are commercially available, and no further chemical modification is needed for SABRE in sharp contrast to hydrogenative pH_2-based hyperpolarization approaches that require suitable unsaturated molecular precursors.[6,7] Additionally, as a result of the low cost and simplicity of SABRE hardware, this approach can be widely available to researchers. Considering recent advances on rapidly extracting SABRE HP pyruvate from methanol into catalyst-free aqueous solution,[13,33] the first preclinical metabolic MRI studies using this technique appear on the near horizon.

In conclusion, we have presented an efficient and rapid approach using rf SLIC and static microtesla fields to produce ^{13}C-hyperpolarized pyruvate using SABRE. While $P_{^{13}C}$ values for both C1 and C2 in protonated pyruvate were similar to levels reached with SABRE-SHEATH, SLIC performed substantially better for the deuterated isotopologue pyruvate-d_3, yielding $P_{^{13}C}$ = 22% for C1 and $P_{^{13}C}$ = 6% for C2. These polarizations are approximately 2 and 6 times higher than those previously reported for protonated SABRE-polarized [1-^{13}C]- and [2-^{13}C]pyruvate. We attribute this improvement to deuteration reducing the degree of intramolecular dipole−dipole relaxation, which prolongs the ^{13}C polarization lifetimes. This strategy is made possible with SLIC, because the microtesla fields employed prevent the deuterons from strongly coupling to the ^{13}C nuclei and acting as a quadrupolar relaxation sink. This is an important observation that we envision adapting to other deuterated compounds to widen the portfolio of SABRE-polarized agents or to enhance their polarization levels.

We have demonstrated this technique for pyruvate, a key metabolite and the most promising HP MRI agent known to date. Experimental parameter optimization may improve the SLIC-SABRE polarizations even further. Both the pyruvate concentration and polarization levels achieved here are sufficient for biomedical applications, and the prolonged polarization lifetimes are promising.[7] We expect this approach to have an important impact on preclinical HP MRI with pyruvate-d_3, facilitating more widespread research and applications.

https://doi.org/10.1021/acs.jpclett.3c00707
J. Phys. Chem. Lett. 2023, 14, 5305−5309

■ ASSOCIATED CONTENT

Supporting Information

The Supporting Information is available free of charge at https://pubs.acs.org/doi/10.1021/acs.jpclett.3c00707.

Additional experimental details, materials, and methods, including photographs of extracted solutions (PDF)

■ AUTHOR INFORMATION

Corresponding Authors

Andreas B. Schmidt − *Division of Medical Physics, Department of Radiology, Medical Center, Faculty of Medicine, University of Freiburg, Freiburg 79106, Germany; German Cancer Consortium (DKTK), Partner Site Freiburg, Freiburg and German Cancer Research Center (DKFZ), Heidelberg 69120, Germany; Department of Chemistry, Integrative Biosciences (Ibio), Karmanos Cancer Institute (KCI), Wayne State University, Detroit, Michigan 48202, United States;* orcid.org/0000-0001-8944-7463; Email: andreas.schmidt@uniklinik-freiburg.de

Stephan Knecht − *NVision Imaging Technologies GmbH, 89081 Ulm, Germany;* orcid.org/0000-0002-8487-4324; Email: stephan@nvision-imaging.com

Authors

James Eills − *Institute for Bioengineering of Catalonia, Barcelona Institute of Science and Technology, 08028 Barcelona, Spain;* orcid.org/0000-0001-8468-6860

Laurynas Dagys − *NVision Imaging Technologies GmbH, 89081 Ulm, Germany;* orcid.org/0000-0003-4935-6115

Martin Gierse − *NVision Imaging Technologies GmbH, 89081 Ulm, Germany;* orcid.org/0000-0002-8187-5903

Michael Keim − *NVision Imaging Technologies GmbH, 89081 Ulm, Germany*

Sebastian Lucas − *NVision Imaging Technologies GmbH, 89081 Ulm, Germany*

Michael Bock − *Division of Medical Physics, Department of Radiology, Medical Center, Faculty of Medicine, University of Freiburg, Freiburg 79106, Germany*

Ilai Schwartz − *NVision Imaging Technologies GmbH, 89081 Ulm, Germany*

Maxim Zaitsev − *Division of Medical Physics, Department of Radiology, Medical Center, Faculty of Medicine, University of Freiburg, Freiburg 79106, Germany*

Eduard Y. Chekmenev − *Department of Chemistry, Integrative Biosciences (Ibio), Karmanos Cancer Institute (KCI), Wayne State University, Detroit, Michigan 48202, United States;* orcid.org/0000-0002-8745-8801

Complete contact information is available at: https://pubs.acs.org/10.1021/acs.jpclett.3c00707

Notes

The authors declare the following competing financial interest(s): The following authors are employees of NVision Imaging Technologies GmbH: Laurynas Dagys, Martin Gierse, Michael Keim, Sebastian Lucas, Ilai Schwartz, and Stephan Knecht. Eduard Y. Chekmenev holds a stake of ownership in XeUS Technologies, Ltd. and serves on the scientific advisory board of Visma Life Sciences LLC.

■ ACKNOWLEDGMENTS

Research reported in this publication was supported by the German Federal Ministry of Education and Research (BMBF) in the funding program "Quantum Technologies—From Basic Research to Market" under the Project "QuE-MRT" (contract 13N16448), the German Cancer Consortium (DKTK), B.E.S.T. Fluidsysteme GmbH / Swagelok Stuttgart, and the German Research Foundation (DFG SCHM 3694/1-1, SCHM 3694/2-1, and SFB1479). This project has received funding from the European Union's Horizon 2020 Research and Innovation Programme under the Marie Skłodowska-Curie Grant Agreement 101063517. Eduard Y. Chekmenev thanks National Science Foundation (NSF) CHE-1904780. Andreas B. Schmidt and Eduard Y. Chekmenev thank Wayne State University for a postdoctoral fellow award.

■ ABBREVIATIONS USED

dDNP, dissolution dynamic nuclear polarization; HP, hyperpolarized; LIGHT-SABRE, low-irradiation generation of high tesla-SABRE; MRI, magnetic resonance imaging; pH_2, parahydrogen; rf, radio frequency; SABRE, signal amplification by reversible exchange; SHEATH, in shield enables alignment transfer to heteronuclei; SLIC, spin-lock induced crossing

■ REFERENCES

(1) Wang, Z. J.; Ohliger, M. A.; Larson, P. E.; Gordon, J. W.; Bok, R. A.; Slater, J.; Villanueva-Meyer, J. E.; Hess, C. P.; Kurhanewicz, J.; Vigneron, D. B. Hyperpolarized ^{13}C MRI: State of the Art and Future Directions. *Radiology* **2019**, *291* (2), 273.

(2) Chowdhury, R.; Mueller, C. A.; Smith, L.; Gong, F.; Papoutsaki, M.-V.; Rogers, H.; Syer, T.; Singh, S.; Brembilla, G.; Retter, A.; Bullock, M.; Caselton, L.; Mathew, M.; Dineen, E.; Parry, T.; Hennig, J.; von Elverfeldt, D.; Schmidt, A. B.; Hövener, J.-B.; Emberton, M.; Atkinson, D.; Bainbridge, A.; Gadian, D. G.; Punwani, S. Quantification of Prostate Cancer Metabolism Using 3D Multiecho BSSFP and Hyperpolarized [1-^{13}C]Pyruvate: Metabolism Differs Between Tumors of the Same Gleason Grade. *J. Magn. Reson. Imaging* **2023**, *57* (6), 1865−1875.

(3) Skinner, J. G.; Menichetti, L.; Flori, A.; Dost, A.; Schmidt, A. B.; Plaumann, M.; Gallagher, F. A.; Hövener, J.-B. Metabolic and Molecular Imaging with Hyperpolarised Tracers. *Mol. Imaging Biol.* **2018**, *20* (6), 902−918.

(4) Chung, B. T.; Chen, H.-Y.; Gordon, J.; Mammoli, D.; Sriram, R.; Autry, A. W.; Le Page, L. M.; Chaumeil, M. M.; Shin, P.; Slater, J.; Tan, C. T.; Suszczynski, C.; Chang, S.; Li, Y.; Bok, R. A.; Ronen, S. M.; Larson, P. E. Z.; Kurhanewicz, J.; Vigneron, D. B. First Hyperpolarized [2-^{13}C]Pyruvate MR Studies of Human Brain Metabolism. *J. Magn. Reson.* **2019**, *309*, 106617.

(5) Ardenkjær-Larsen, J. H.; Fridlund, B.; Gram, A.; Hansson, G.; Hansson, L.; Lerche, M. H.; Servin, R.; Thaning, M.; Golman, K. Increase in Signal-to-Noise Ratio of > 10,000 Times in Liquid-State NMR. *Proc. Natl. Acad. Sci. U. S. A.* **2003**, *100* (18), 10158−10163.

(6) Schmidt, A. B.; Bowers, C. R.; Buckenmaier, K.; Chekmenev, E. Y.; de Maissin, H.; Eills, J.; Ellermann, F.; Glöggler, S.; Gordon, J. W.; Knecht, S.; Koptyug, I. V.; Kuhn, J.; Pravdivtsev, A. N.; Reineri, F.; Theis, T.; Them, K.; Hövener, J.-B. Instrumentation for Hydrogenative Parahydrogen-Based Hyperpolarization Techniques. *Anal. Chem.* **2022**, *94* (1), 479−502.

(7) Hövener, J.-B.; Pravdivtsev, A. N.; Kidd, B.; Bowers, C. R.; Glöggler, S.; Kovtunov, K. V.; Plaumann, M.; Katz-Brull, R.; Buckenmaier, K.; Jerschow, A.; Reineri, F.; Theis, T.; Shchepin, R. V.; Wagner, S.; Bhattacharya, P.; Zacharias, N. M.; Chekmenev, E. Y. Parahydrogen-Based Hyperpolarization for Biomedicine. *Angew. Chem., Int. Ed.* **2018**, *57* (35), 11140−11162.

(8) Adams, R. W.; Aguilar, J. A.; Atkinson, K. D.; Cowley, M. J.; Elliott, P. I. P.; Duckett, S. B.; Green, G. G. R.; Khazal, I. G.; López-Serrano, J.; Williamson, D. C. Reversible Interactions with Para-Hydrogen Enhance NMR Sensitivity by Polarization Transfer. *Science* **2009**, *323* (5922), 1708−1711.

(9) Cowley, M. J.; Adams, R. W.; Atkinson, K. D.; Cockett, M. C. R.; Duckett, S. B.; Green, G. G. R.; Lohman, J. A. B.; Kerssebaum, R.; Kilgour, D.; Mewis, R. E. Iridium N-Heterocyclic Carbene Complexes as Efficient Catalysts for Magnetization Transfer from *para*-Hydrogen. *J. Am. Chem. Soc.* **2011**, *133* (16), 6134−6137.
(10) Iali, W.; Roy, S. S.; Tickner, B. J.; Ahwal, F.; Kennerley, A. J.; Duckett, S. B. Hyperpolarising Pyruvate through Signal Amplification by Reversible Exchange (SABRE). *Angew. Chem.* **2019**, *131* (30), 10377−10381.
(11) TomHon, P.; Abdulmojeed, M.; Adelabu, I.; Nantogma, S.; Kabir, M. S. H.; Lehmkuhl, S.; Chekmenev, E. Y.; Theis, T. Temperature Cycling Enables Efficient ^{13}C SABRE-SHEATH Hyperpolarization and Imaging of [1-^{13}C]-Pyruvate. *J. Am. Chem. Soc.* **2022**, *144* (1), 282−287.
(12) Adelabu, I.; TomHon, P.; Kabir, M. S. H.; Nantogma, S.; Abdulmojeed, M.; Mandzhieva, I.; Ettedgui, J.; Swenson, R. E.; Krishna, M. C.; Theis, T.; Goodson, B. M.; Chekmenev, E. Y. Order-Unity ^{13}C Nuclear Polarization of [1-^{13}C]Pyruvate in Seconds and the Interplay of Water and SABRE Enhancement. *ChemPhysChem* **2022**, *23* (2), No. e202100839.
(13) Schmidt, A. B.; de Maissin, H.; Adelabu, I.; Nantogma, S.; Ettedgui, J.; TomHon, P.; Goodson, B. M.; Theis, T.; Chekmenev, E. Y. Catalyst-Free Aqueous Hyperpolarized [1-^{13}C]Pyruvate Obtained by Re-dissolution Signal Amplification by Reversible Exchange. *ACS Sens.* **2022**, *7* (11), 3430−3439.
(14) Ivanov, K. L.; Pravdivtsev, A. N.; Yurkovskaya, A. V.; Vieth, H.-M.; Kaptein, R. The Role of Level Anti-Crossings in Nuclear Spin Hyperpolarization. *Prog. Nucl. Magn. Reson. Spectrosc.* **2014**, *81*, 1−36.
(15) Theis, T.; Truong, M. L.; Coffey, A. M.; Shchepin, R. V.; Waddell, K. W.; Shi, F.; Goodson, B. M.; Warren, W. S.; Chekmenev, E. Y. Microtesla SABRE Enables 10% Nitrogen-15 Nuclear Spin Polarization. *J. Am. Chem. Soc.* **2015**, *137* (4), 1404−1407.
(16) Zhivonitko, V. V.; Skovpin, I. V.; Koptyug, I. V. Strong ^{31}P Nuclear Spin Hyperpolarization Produced via Reversible Chemical Interaction with Parahydrogen. *Chem. Commun.* **2015**, *51* (13), 2506−2509.
(17) Barskiy, D. A.; Shchepin, R. V.; Tanner, C. P. N.; Colell, J. F. P.; Goodson, B. M.; Theis, T.; Warren, W. S.; Chekmenev, E. Y. The Absence of Quadrupolar Nuclei Facilitates Efficient ^{13}C Hyperpolarization via Reversible Exchange with Parahydrogen. *ChemPhysChem* **2017**, *18* (12), 1493−1498.
(18) Lindale, J. R.; Eriksson, S. L.; Tanner, C. P. N.; Zhou, Z.; Colell, J. F. P.; Zhang, G.; Bae, J.; Chekmenev, E. Y.; Theis, T.; Warren, W. S. Unveiling Coherently Driven Hyperpolarization Dynamics in Signal Amplification by Reversible Exchange. *Nat. Commun.* **2019**, *10* (1), 395.
(19) Pravdivtsev, A. N.; Kempf, N.; Plaumann, M.; Bernarding, J.; Scheffler, K.; Hövener, J.-B.; Buckenmaier, K. Coherent Evolution of Signal Amplification by Reversible Exchange in Two Alternating Fields (Alt-SABRE). *ChemPhysChem* **2021**, *22* (23), 2381−2386.
(20) Eriksson, S. L.; Lindale, J. R.; Li, X.; Warren, W. S. Improving SABRE Hyperpolarization with Highly Nonintuitive Pulse Sequences: Moving beyond Avoided Crossings to Describe Dynamics. *Sci. Adv.* **2022**, *8* (11), No. eabl3708.
(21) Nantogma, S.; Eriksson, S. L.; Adelabu, I.; Mandzhieva, I.; Browning, A.; TomHon, P.; Warren, W. S.; Theis, T.; Goodson, B. M.; Chekmenev, E. Y. Interplay of Near-Zero-Field Dephasing, Rephasing, and Relaxation Dynamics and [1-^{13}C]Pyruvate Polarization Transfer Efficiency in Pulsed SABRE-SHEATH. *J. Phys. Chem. A* **2022**, *126* (48), 9114−9123.
(22) Pravdivtsev, A. N.; Yurkovskaya, A. V.; Zimmermann, H.; Vieth, H.-M.; Ivanov, K. L. Enhancing NMR of Insensitive Nuclei by Transfer of SABRE Spin Hyperpolarization. *Chem. Phys. Lett.* **2016**, *661*, 77−82.
(23) Knecht, S.; Kiryutin, A. S.; Yurkovskaya, A. V.; Ivanov, K. L. Re-Polarization of Nuclear Spins Using Selective SABRE-INEPT. *J. Magn. Reson.* **2018**, *287*, 10−14.
(24) DeVience, S. J.; Walsworth, R. L.; Rosen, M. S. Preparation of Nuclear Spin Singlet States Using Spin-Lock Induced Crossing. *Phys. Rev. Lett.* **2013**, *111* (17), 173002.
(25) Theis, T.; Truong, M.; Coffey, A. M.; Chekmenev, E. Y.; Warren, W. S. LIGHT-SABRE Enables Efficient in-Magnet Catalytic Hyperpolarization. *J. Magn. Reson.* **2014**, *248*, 23−26.
(26) Pravdivtsev, A. N.; Skovpin, I. V.; Svyatova, A. I.; Chukanov, N. V.; Kovtunova, L. M.; Bukhtiyarov, V. I.; Chekmenev, E. Y.; Kovtunov, K. V.; Koptyug, I. V.; Hövener, J.-B. Chemical Exchange Reaction Effect on Polarization Transfer Efficiency in SLIC-SABRE. *J. Phys. Chem. A* **2018**, *122* (46), 9107−9114.
(27) Knecht, S.; Kiryutin, A. S.; Yurkovskaya, A. V.; Ivanov, K. L. Efficient Conversion of Anti-Phase Spin Order of Protons into ^{15}N Magnetisation Using SLIC-SABRE. *Mol. Phys.* **2019**, *117* (19), 2762−2771.
(28) Svyatova, A.; Skovpin, I. V.; Chukanov, N. V.; Kovtunov, K. V.; Chekmenev, E. Y.; Pravdivtsev, A. N.; Hövener, J.-B.; Koptyug, I. V. ^{15}N MRI of SLIC-SABRE Hyperpolarized ^{15}N-Labelled Pyridine and Nicotinamide. *Chem. - Eur. J.* **2019**, *25* (36), 8465−8470.
(29) Pravdivtsev, A. N.; Buckenmaier, K.; Kempf, N.; Stevanato, G.; Scheffler, K.; Engelmann, J.; Plaumann, M.; Koerber, R.; Hovener, J.-B.; Theis, T. LIGHT-SABRE Hyperpolarizes 1- ^{13} C-Pyruvate Continuously without Magnetic Field Cycling. *J. Phys. Chem. C* **2023**, *127* (14), 6744−6753.
(30) Berner, S.; Schmidt, A. B.; Zimmermann, M.; Pravdivtsev, A. N.; Glöggler, S.; Hennig, J.; von Elverfeldt, D.; Hövener, J.-B. SAMBADENA Hyperpolarization of ^{13}C-Succinate in an MRI: Singlet-Triplet Mixing Causes Polarization Loss. *ChemistryOpen* **2019**, *8* (6), 728−736.
(31) Marshall, A.; Salhov, A.; Gierse, M.; Müller, C.; Keim, M.; Lucas, S.; Parker, A.; Scheuer, J.; Vassiliou, C.; Neumann, P.; Jelezko, F.; Retzker, A.; Blanchard, J. W.; Schwartz, I.; Knecht, S. Radio-Frequency Sweeps at Microtesla Fields for Parahydrogen-Induced Polarization of Biomolecules. *J. Phys. Chem. Lett.* **2023**, *14* (8), 2125−2132.
(32) Taglang, C.; Korenchan, D. E.; von Morze, C.; Yu, J.; Najac, C.; Wang, S.; Blecha, J. E.; Subramaniam, S.; Bok, R.; VanBrocklin, H. F.; Vigneron, D. B.; Ronen, S. M.; Sriram, R.; Kurhanewicz, J.; Wilson, D. M.; Flavell, R. R. Late-Stage Deuteration of ^{13}C-Enriched Substrates for T_1 Prolongation in Hyperpolarized ^{13}C MRI. *Chem. Commun.* **2018**, *54* (41), 5233−5236.
(33) de Maissin, H.; Groß, P.; Mohiuddin, O.; Weigt, M.; Nagel, L.; Herzog, M.; Wang, Z.; Willing, R.; Reichardt, W.; Pichotka, M.; Heß, L.; Reinheckel, T.; Jessen, H.; Zeiser, R.; Bock, M.; Elverfeldt, D. von; Zaitsev, M.; Korchak, S.; Glöggler, S.; Hövener, J.-B.; Chekmenev, E.; Schilling, F.; Knecht, S.; Schmidt, A. B. *In Vivo* Metabolic Imaging of [1-^{13}C]Pyruvate-d_3 Hyperpolarized by Reversible Exchange with Parahydrogen. *ChemRxiv* **2023**, DOI: 10.26434/chemrxiv-2023-9trxb.
(34) Westheimer, F. H. The Magnitude of the Primary Kinetic Isotope Effect for Compounds of Hydrogen and Deuterium. *Chem. Rev.* **1961**, *61* (3), 265−273.
(35) Bednarik, P.; Goranovic, D.; Svatkova, A.; Niess, F.; Hingerl, L.; Strasser, B.; Deelchand, D. K.; Spurny-Dworak, B.; Krssak, M.; Trattnig, S.; Hangel, G.; Scherer, T.; Lanzenberger, R.; Bogner, W. ^{1}H Magnetic Resonance Spectroscopic Imaging of Deuterated Glucose and of Neurotransmitter Metabolism at 7 T in the Human Brain. *Nat. Biomed. Eng.* **2023**, 1−13.
(36) Funk, A. M.; Wen, X.; Hever, T.; Maptue, N. R.; Khemtong, C.; Sherry, A. D.; Malloy, C. R. Effects of Deuteration on Transamination and Oxidation of Hyperpolarized ^{13}C-Pyruvate in the Isolated Heart. *J. Magn. Reson.* **2019**, *301*, 102−108.

https://doi.org/10.1021/acs.jpclett.3c00707
J. Phys. Chem. Lett. 2023, 14, 5305−5309